

Electrochemical Evaluation of Ni/RuO₂ and Ni/RuO₂/Mixed-Metal Oxide Coatings Electrodes toward Hydrogen Evolution Reaction in Alkaline Medium

Mir Ghasem Hosseini ^{*,a,b}, Esmaeel Ariankhah^a

^aElectrochemistry Research Laboratory, Department of Physical Chemistry, Chemistry Faculty, University of Tabriz, Tabriz, Iran

^bEngineering Faculty, Department of Materials Science and Nanotechnology, Near East

Article history:

Received: 30/Jun/2016

Received in revised form: -

Accepted: 28/Aug/2016

Abstract

Ni/RuO₂ electrode was fabricated by electrochemical deposition from an acidic RuCl₃ solution at room temperature, then annealing at 120°C for 150 min. Morphology characterization revealed a mud-crack structure and electrochemical investigations of Ni/RuO₂ and Ni bare substrate indicated more activity of Ni/RuO₂ toward hydrogen evolution reaction. Afterward, RuO₂-TiO₂ (20-80), RuO₂-TiO₂-IrO₂ (20-60-20) and RuO₂-TiO₂-Ta₂O₅ (20-60-20) mol. % were constructed by sol gel and thermal decomposition at 450°C on previously prepared Ni/RuO₂ substrates. SEM micrographs showed the most roughness for RuO₂-TiO₂-IrO₂ coating. XRD analysis revealed the formation of solid solution structures between RuO₂ by IrO₂ and Ta₂O₅. Electrochemical studies, including activity and stability studies also revealed the excellent performance for RuO₂-TiO₂-IrO₂ due to its more surface roughness and also stabilizing effect of IrO₂ and RuO₂ on each other.

Keywords: hydrogen evolution reaction, mixed metal oxide coatings, roughness, accelerated life test, electrochemical impedanc

1. Introduction

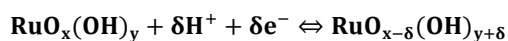
Hydrogen evolution reaction (HER), as one of interesting research fields in electrochemistry, has been studied extremely in recent decades. The pollutant nature of fossil fuels and global warming due to the yields of their burning reaction have led to considering of Hydrogen as an alternative green and renewable energy carrier for the future, especially in the growing craft of hydrogen fuel cells [1]. Attempts on the replacement of combustion engines with PEM fuel cells in transportation vehicles or making hybrid forms

have highlighted the importance of the economical and large scale production of hydrogen [2, 3]. Hydrogen production can be conducted through many ways, among which the most important cases to consider, involve steam reforming of hydrocarbons, partial oxidation of coal and oils, thermolysis of water at very high temperatures and electrolysis of water [4].

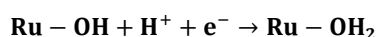
*.Corresponding Author: E-mail address: mg-hosseini@tabrizu.ac.ir; Tel.: +(98)4133393138

Despite the decline of oils and hydrocarbon sources, the unwanted effects of reforming and partial oxidation outputs like carbon dioxide are challenging issue [5]. Electrolysis of water, as a familiar method, has a less pollutant nature among the aforementioned ways [6]. It can be conducted in both acidic and alkaline mediums [7-9]. In alkaline mediums, water reduces and produces soda and hydrogen gas under an impressed constant current at the cathode compartment which can be a metal, alloy and hybrid coatings including organic and inorganic materials on a given substrate. Platinum is a talented metal for electrocatalyzing of HER. Catalytic activity of Platinum in acidic medium is much more than alkaline [10-12]. However platinum is an expensive metal and isn't active as well as expected in alkaline mediums. Nickel also has been considered as a suitable substrate in these electrodes particularly in alkaline mediums. Although the activity of nickel toward HER is less in comparison with metals like Pt, Au and Ir but, it has needed stability in alkaline medium. To overcome the lower activity several ways have been proposed and investigated by many authors that are summarized at following: 1) Alloying Ni with other metals as Mo, Co and Fe [13, 14]. 2) Increasing the surface; as implements at raney-Ni compounds; Ni-Al or Ni-Zn coatings have been developed in this way [15, 16]. 3) Covering Ni surface by a given, suitable coatings. These coatings can be constructed from sulphide, nitride, carbide of one or more transition metal [17-19] and also typical transition metal oxides or mixed metal oxide (MMO) of noble metals [20-23] in which there is an enormous inherent activity toward HER. Coatings with high activity in HER which embeds on the Ni substrate not only should compensate the activity of Ni but should have desired stability in industrial conditions. IrO₂ and

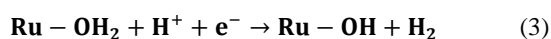
RuO₂ have some basic advantages needed to application on hydrogen evolving cathodes include high conductivity, thermal stability and reversible redox features [24]. They have been studied as hydrogen evolving catalyst coatings in acidic mediums [25, 26]. The surface of such electrodes with MMO coatings prepared at low temperature is full of hydroxyl groups. These groups are the active sites of electrode for catalyzing HER. Many authors have confirmed that when the surface of such electrodes polarizes to negative potentials (cathodic polarization) a reversible proton-electron faradaic reaction, between surface and electrolyte transacts, such as dedicated below, that is not only the responsible for electrocatalytic activity of RuO₂ or IrO₂ in HER but the pseudocapacitance properties of such materials [23].



(1) Furthermore, IrO₂ has faradaic redox equilibrium on its surface at aqueous solution similar to reaction 1. According to the literature HER proceed by two proposed mechanisms on Hydrous RuO₂ and IrO₂. The first mechanism which has been proposed by Boodts and Trasatti encompasses three steps that begin by reduction of hydroxyl sites at the surface, followed by formation of hydride and finally evolution of hydrogen molecule [27]. Chen et al. [25] proposed a Volmer-Heyrosky type mechanism based on their ac impedance studies and many other authors approved the same approach on their work [28]. This mechanism is shown at the equations 2 and 3.



(2)



(3)

Although in the literature the coatings based on IrO₂, RuO₂ and their mixtures have been accepted evidently as active materials for HER but there is a lack of study on the application of mixed metal oxide coatings for HER. In this work, we made Ni/RuO₂

electrodes by electrodeposition of a thin layer of RuO₂ from RuCl₃ at room temperature on Ni substrate. The film was then heated at 120°C to form a rigid and stable coating. After evaluation of the electrochemical properties of this coating, three different compositions of mixed metal oxide coatings including RuO₂, TiO₂, IrO₂ and Ta₂O₅ were applied on previously prepared Ni/RuO₂ electrodes. Double layer capacitance and electrocatalytic activity of these electrodes toward HER were investigated by cyclic voltammetry, polarization and electrochemical impedance spectroscopy techniques. As well as stability of coatings was evaluated by constant current density electrolysis.

2. Experimental procedure

2.1. Materials and Methods

Analytical grade of anhydrous salts of IrCl₃, RuCl₃, TaCl₅, n-butanol and Ti(OBu)₄ were purchased from Merck and HCl (36%) from Dae Jung company. Characterization of electrochemically prepared Ni/RuO₂ substrate and sol gel derived coatings were conducted through SEM and EDX analysis by field emission scanning electron microscope (MR1A3, TESCAN, Czech Republic) equipped with EDX analyzer. To investigation of the structure of the coatings prepared by sol gel procedure and annealing at 450°C XRD patterns achieved by X-Ray diffractometer (D8 ADVANCE, Germany) operated at 40kV/40mA with K α of copper. Peak analysis of all XRD patterns was conducted by PANalytical XPert HighScore software.

2.2. Preparation of Ni/RuO₂ substrate

Three Ni mesh substrates with the 1cm² geometric areas were degreased in a 40 g.L⁻¹ solution of soda. After rinsing in double distilled water and drying at oven, they were etched in a vol. 15% HCl solution at room temperature. RuO₂ cathodically electrodeposited on the pretreated Ni substrates in 5 mmol.L⁻¹ acidic RuCl₃ solution. Electrodeposition

carried out by application of 25mA.cm⁻² for 30 minutes at room temperature and pH=2. After electrodeposition, these three electrodes were transferred to furnace and heated at 120°C for 150 minutes to achieve dense and rigid

2.3. Preparation of TiO₂-RuO₂, TiO₂-RuO₂-IrO₂, TiO₂-RuO₂-Ta₂O₅ coatings on Ni/RuO₂ substrate

Needed solutions for painting of coatings were prepared by addition of given values of chloride salts of metals to n-butanol solvent. For this propose, three different solutions were prepared which were named as A, B and C. Solution A was a mixture of RuCl₃, n-butanol, and HCl; the second, B, contained RuCl₃, IrCl₄, n-butanol and HCl; and the third, C, included RuCl₃, TaCl₅, n-butanol and HCl. After preparation of A, B and C, they were stirred for 1 hour at room temperature. Then To achieve the final solutions a stoichiometric amount of TiO₂ producer alkoxide reagent; Ti(OBu)₄ was added to A, B and C to produce gel mixtures of Ti-Ru by molar% of (80:20), Ti-Ru-Ir by molar% of (60:20:20) and Ti-Ru-Ta by molar% of (60:20:20). 16 layers of each solution were painted on Ni/RuO₂ substrates in a way that ultimately the amount of coating was 0.05g at all cases and at each painting step the electrode was heated first at 90°C for 20 minutes to removing residual solvent and then at 450°C for 30 min in order to thermal decomposition and crystallization of gels.

2.4 Electrochemical measurements

Electrochemical measurements were carried out by means of EG&G PARSTAT 2263 in a pyrex beaker with three electrode system including a 10cm² platinum plate as counter and standard calomel electrode (SCE) as reference electrode. All experiments were done at room temperature in 1 mol.L⁻¹ NaOH solution except the accelerated stability test in which a 2mol L⁻¹ NaOH solution was utilized. Cyclic voltammetry (CV), tafel polarization and electrochemical impedance spectroscopy (EIS)

techniques were used for electrochemical investigation in this work. Cyclic voltammetry of Ni mesh and electrochemically prepared Ni/RuO₂ substrate obtained at a potential range of -1 to +1 V vs. SCE at the scan rate of 50 mV s⁻¹. For sol gel derived coatings, voltammograms were procured at scan rates of 25, 50, 100 and 200mV.s⁻¹ at the potential range of -1.1 to +0.5 V vs. SCE. All EIS data at this work were achieved at frequency range of 10 mHz to 100 kHz. The potential in which the EIS data were obtained for sol gel derived coatings was -0.85V vs. SCE. Also the all polarization curves obtained at scan rate of 1mV s⁻¹.

3. Results and discussion

3.1 Morphology and structure analysis

RuO₂ film was deposited on Ni substrates by electrochemical route then heated in 120°C to form a rigid structure. Figure 1 shows the SEM micrographs of electrochemically deposited RuO₂ film on Ni substrate. As it was expected, the surface contains cracks due to the heat treatment. By considering fig. 1 the RuO₂ film constitutes two kinds of structures at its surface. One is the background or inner layer which is smooth with narrow cracks and the other is the agglomerations (white points) which have different sizes and have spread out on the entire surface.

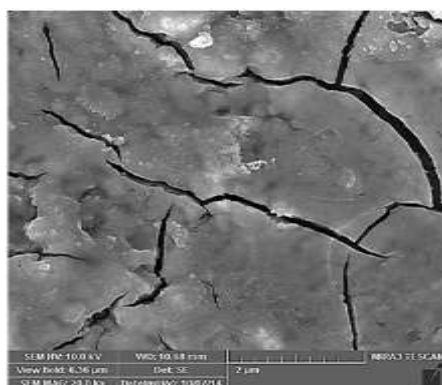


Figure 1. SEM micrographs of Ni/RuO₂ substrate prepared by electrochemical deposition and heating at 120°C.

Existence of cracks proves the formation of RuO₂ because the cracks are the characteristic feature of such oxide coatings. Similar results have been reported by Hu et al. [29] Based on the report of Yoshida et al. the structure of ruthenium oxide at lower annealing temperatures is as RuO₂.nH₂O in which the water content (n) changes by increasing annealing temperature [30]. The SEM micrographs of thermally prepared coatings at 450°C are shown in Figure 2. The figures A and B are relevant to the coating of RuO₂-TiO₂. The surface encompasses the islands (with different size) and the deep cracks like channels which have surrounded the islands.

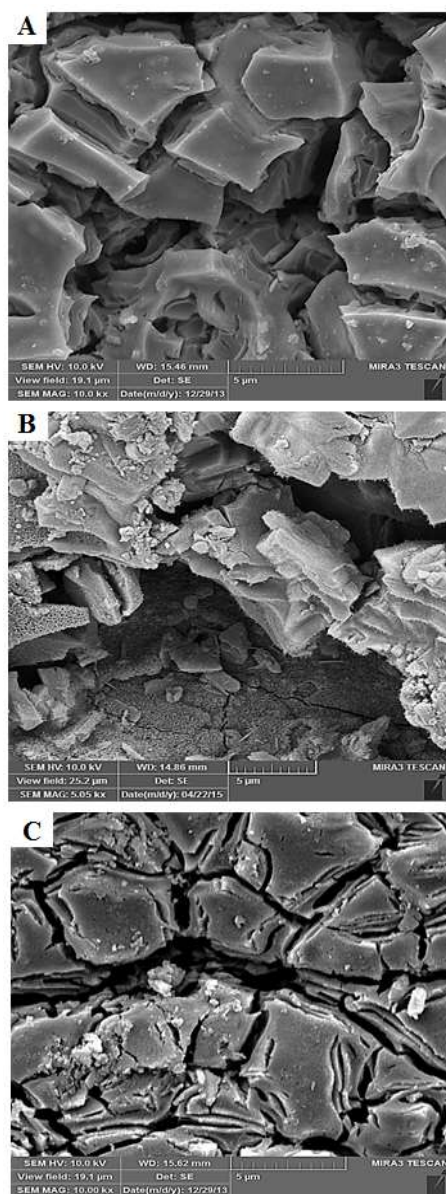


Figure 2. SEM micrographs of coatings prepared by sol-gel procedure and annealing at 450°C A) $\text{RuO}_2\text{-TiO}_2$ (20-80) , B) $\text{RuO}_2\text{-TiO}_2\text{-IrO}_2$ (20-60-20) and C) $\text{RuO}_2\text{-TiO}_2\text{-Ta}_2\text{O}_5$ (20-60-20) mol. % coatings.

The islands are almost flat with no excess aggregates. $\text{RuO}_2\text{-TiO}_2$ has large number of cracks and grooves which are very deep and broad [31]. The figures E and F belong to $\text{RuO}_2\text{-TiO}_2\text{-Ta}_2\text{O}_5$ coating. The islands at this case are slightly smaller than $\text{RuO}_2\text{-TiO}_2$ coating but the basic morphological form is similar at both of the coatings. The main difference between $\text{RuO}_2\text{-TiO}_2$ and $\text{RuO}_2\text{-TiO}_2\text{-Ta}_2\text{O}_5$ coatings is that the second

A

case has a finite quantity of fine pores by the size lower than 200nm on its islands as can be seen in figure 3A.

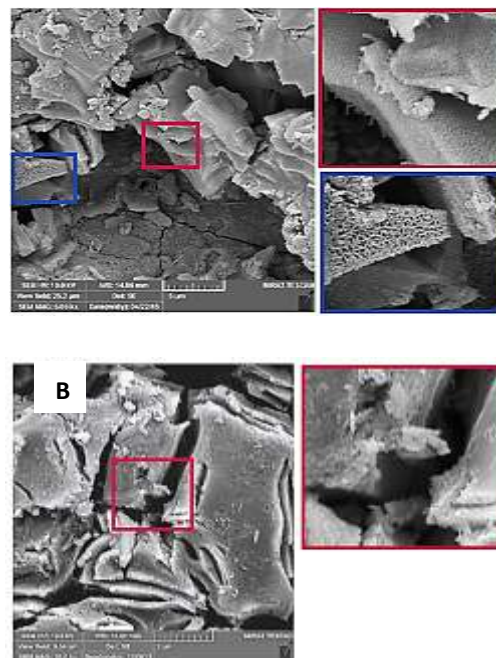


Figure 3. The pores with different shape and size at two different positions on A) $\text{RuO}_2\text{-TiO}_2\text{-IrO}_2$ (20-60-20) and B) $\text{RuO}_2\text{-TiO}_2\text{-Ta}_2\text{O}_5$ (20-60-20) mol. % coatings.

At the case of $\text{RuO}_2\text{-TiO}_2\text{-IrO}_2$ coating addition of IrO_2 has led to change in morphology of the coating. Most of the deep and sharp cracks have leaved narrow lines. Moreover it seems the coating has been delaminated and got a more porous structure through alteration of the cracks by irregular holes in terms of size and shape. Another important note about the coating which contains IrO_2 is that the surface of holes and cracks are scaly with pores even lower than 100 nm. They are shown in figure 3B. These pores cannot be seen ever at $\text{RuO}_2\text{-TiO}_2$ and $\text{RuO}_2\text{-TiO}_2\text{-Ta}_2\text{O}_5$ coatings. For examination of the composition of the coatings prepared by sol-gel and heat treatment at 450°C, Energy dispersive x-ray analysis was implemented and the spectrums were presented in Figure 4. Prior to the analysis a thin film of gold was deposited by chemical vapor deposition route on the all three samples to improvement their conductivity. The peak named as (Au) in Figure 4 is in association

with this film. The elements of each of coatings clearly have been appeared at the relevant spectra. At the fig. 4B the peak characteristic of Ir overlaps with Au however Ir can be recognized.

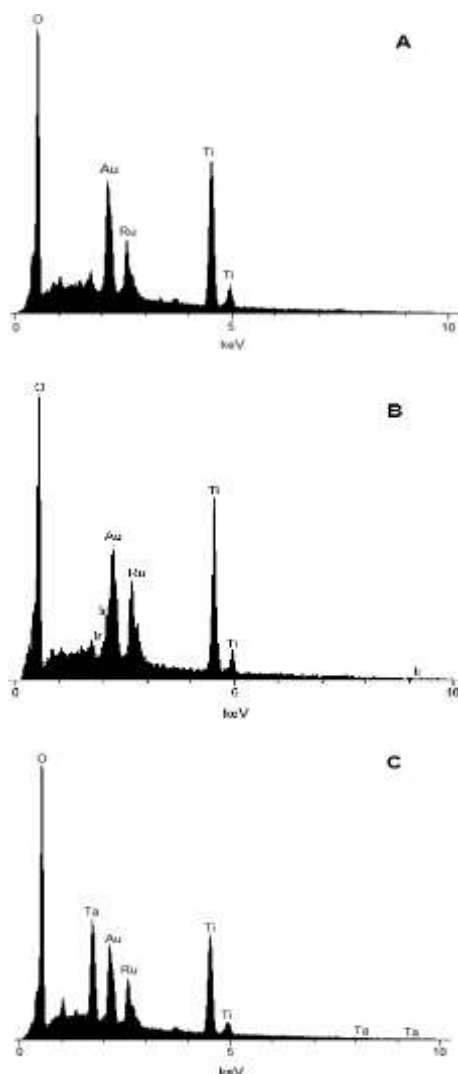


Figure 4. EDX spectra of coatings prepared by sol-gel procedure and annealing at 450°C A) RuO₂-TiO₂ (20-80), B) RuO₂-TiO₂-IrO₂ (20-60-20) and C) RuO₂-TiO₂-Ta₂O₅ (20-60-20) mol. % coatings.

XRD patterns obtained for the coatings prepared by sol gel and thermal decomposition at 450°C are shown in Figure 5. The binary coating of RuO₂-TiO₂ has a complex plan including anatase and rutile forms of TiO₂. At the both patterns of RuO₂-TiO₂-IrO₂ and RuO₂-TiO₂-Ta₂O₅ it can be clearly seen that addition of IrO₂ and Ta₂O₅ has led to change in intensity and width of rutile-type structure peaks. Also the peak deployed at 54° which has rutile characteristic alters

by addition of IrO₂ and Ta₂O₅. It can be resulted from the formation of solid solution structures between RuO₂, TiO₂ and IrO₂ because of similar ion radius between Ru⁴⁺,Ti⁴⁺ and Ru⁴⁺ [32]. Also Ta₂O₅ can contribute at the solid solution structure with RuO₂ and TiO₂ up to 10% [33]. RuO₂ at middle temperatures like 450°C has a crystalline structure but IrO₂ and Ta₂O₅ oxides poorly crystalize and almost remain in their amorphous form [34]. Anatase peaks of TiO₂ clearly are affected by IrO₂ and Ta₂O₅ incorporation to the coatings. Also there is no any sign about existing of peaks representative to existing of metallic material specially Ni.

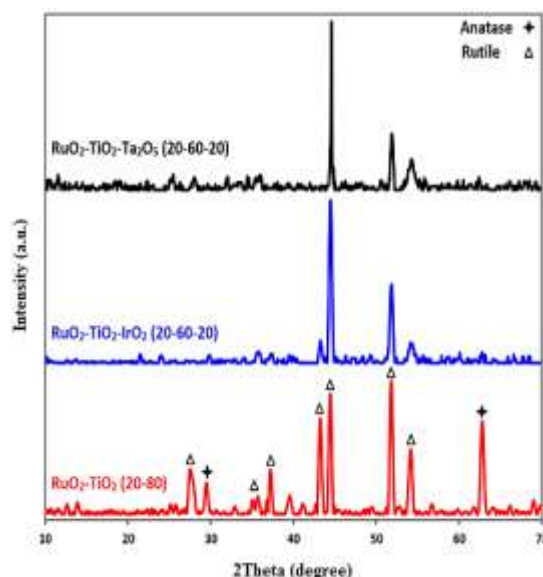


Figure 5. XRD patterns of the coatings prepared with sol gel procedure and annealing at 450°C.

3.2 Electrochemical results

3.2.1 Electrochemical properties of Ni and Ni/RuO₂ substrates

Cyclic voltammograms of Ni substrate and Ni/RuO₂ prepared by cathodic electrodeposition of RuO₂ on pretreated Ni substrate are presented in fig. 6. They were achieved at a scan rate of 50 mV.s⁻¹ in 1 mol.L⁻¹ NaOH solution at 25°C. The shape of voltammograms is mainly different and there is no sign of Ni at the voltammogram of Ni/RuO₂. It implicitly indicates that RuO₂ film fabricated by electrodeposition and then heating at 120°C has a

uniform and integrated structure. Interestingly the shape of cyclic voltammogram of Ni/RuO₂ electrode is very similar to that of Ni/RuO₂ in sulfuric acid medium [35]. There are some differences between the two curves. First the water window at the surface of Ni is about 1.9V however it decreases to near 1.3V at the surface of Ni/RuO₂ electrode. As can be seen in figure 6 the water reduction peak or HER has been revealed near -0.75V vs. SCE on the surface of Ni/RuO₂ electrode however it appears at -1V in the case of Ni bare substrate. Then the HER onset potential has shifted about 250mV to positive potentials. Extension of water window means the poor water oxidation (OER) and reduction (HER) at the surface of Ni substrate. Second matter is that the reduction and oxidation currents in the case of Ni/RuO₂ are very larger than bare Ni. These large currents implicates on more surface properties and favorable sites on the surface of Ni/RuO₂ electrode.

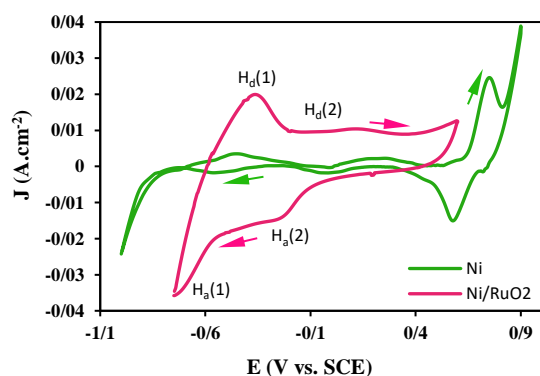


Figure 6. Cyclic voltammograms of Ni and Ni/RuO₂ at scan rate of 50 mV.s⁻¹ in a 1 mol L⁻¹ NaOH solution. (a: adsorption and d: desorption).

According to the figure 6 there are two kinds of surface sites on Ni/RuO₂ electrode which have marked as pairs of H_a(1)-H_d(1) and H_a(2)-H_d(2) [35]. Linear sweep voltammetry was conducted to more of the Ni/RuO₂ activity toward HER. Figure 7A shows the IR corrected linear sweep voltammograms of Ni and Ni/RuO₂ electrodes achieved at 1mV.s⁻¹ scan rate in 1mol.L⁻¹ NaOH. The slope of change of current density proportion to potential change ($\frac{dJ}{dE}$) is higher

for Ni/RuO₂. In other words, by a given change in potential, the observed current density is higher for Ni/RuO₂ than the Ni substrate. It is related to intrinsic activity of RuO₂ in electrocatalyzing of HER and depends on water adsorption-desorption activation energy and strength of adsorption bond between water and surface sites. According to above mentioned results Ni/RuO₂ is more active toward HER than bare Ni. Also By taking into account of the equilibrium potentials of -0.6V and -0.839V vs. SCE respectively for Ni/RuO₂ and Ni bare substrate according to the tafel polarization curves at figure 7B the needed overpotential to passing 1mA cm⁻² current density from the electrodes is 19 and 121mV respectively for Ni/RuO₂ and Ni electrodes. In addition the measured tafel slope for Ni/RuO₂ is 42 mV dec⁻¹ at lower and 225 mV dec⁻¹ at higher current densities for Ni/RuO₂ electrode [23, 36]. A single tafel slope of 72 mV dec⁻¹ was observed for Ni bare substrate at all potential range.

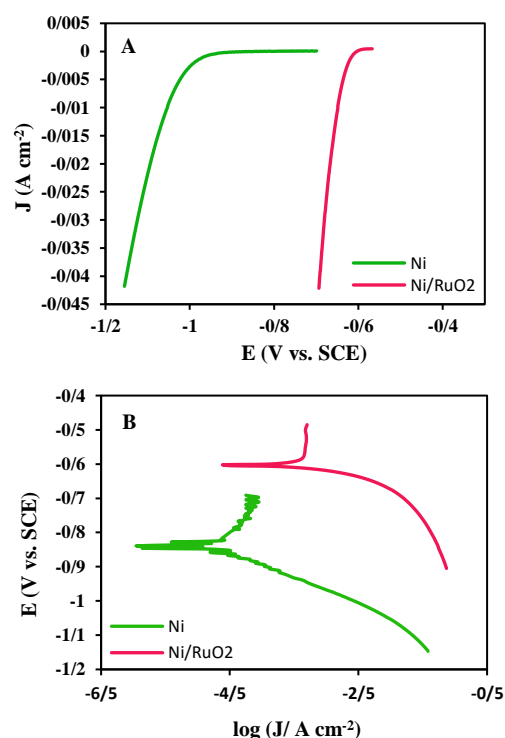


Figure 7. A) Linear sweep voltammetry and B) Tafel polarization curves of Ni and Ni/RuO₂ at scan rate of 1 mV.s⁻¹ in a 1 mol L⁻¹ NaOH solution.

Regarding to the higher activity of Ni/RuO₂ electrode, it was used as substrate and three different kinds of mixed metal oxide coatings encompassing RuO₂-TiO₂ (20-80), RuO₂-TiO₂-IrO₂ (20-60-20) and RuO₂-TiO₂-Ta₂O₅ (20-60-20) mol. % were fabricated by sol gel and thermal decomposition at 450°C on it.

3.2.2 Electrochemical properties of Ni/RuO₂/RuO₂-TiO₂, Ni/RuO₂/RuO₂-TiO₂-IrO₂, Ni/RuO₂/RuO₂-TiO₂-Ta₂O₅ electrodes

Mixed metal oxide coatings, composed of noble metal oxides, were synthesized by a mixed method encompassing sol gel procedure and thermal decomposition at 450°C. The electrochemical activity of coatings toward HER was first investigated by electrochemical impedance spectroscopy as a powerful tool for assessment of both resistance and capacitance features of an electrochemical system. In this regard, impedance spectroscopy was done in a 1mol.L⁻¹ NaOH solution at 25°C. The potential was adjusted at -0.85V vs. SCE whereas the amplitude of applied current oscillation was 10mA. Fig. 7 shows the obtained Nyquist diagrams. This type of two time constant Nyquist diagrams already has been achieved for hydrogen evolving metal oxide electrodes by many authors [23, 28]. Single CPE model also has been used in some cases [20]. The obtained diagrams at this work have two overlapping semicircles; one smaller at high frequency and the other big and at low. The first semicircle at high frequency belongs to the interface of substrate/coating and the second at low frequency pertains to the interface of coating/electrolyte. The results were fitted to an electrochemical equivalent circuit (EEC) consist of two nested randles cells. The EEC shape is shown inside the figure 8. R1 is the sum of solution resistance with all physical connection resistances. R2 is the resistance of coating and R3 is the charge transfer resistance of hydrogen evolution reaction. CPE1 and CPE2 are the constant phase elements respectively for the substrate/coating and

coating/electrolyte interfaces and their impedance is given as following:

$$Z_{CPE} = \frac{1}{T(j\omega)^n}$$

(4) Utilization of CPE instead

of C_{dl} is more proper in the cases like the present work that the surface of electrodes is rough and heterogenic [20, 28]. The parameter of T has a constant value which is related to the double layer capacitance through equation (5) and n is a unit less parameter corresponds to the depression angle of semicircle.

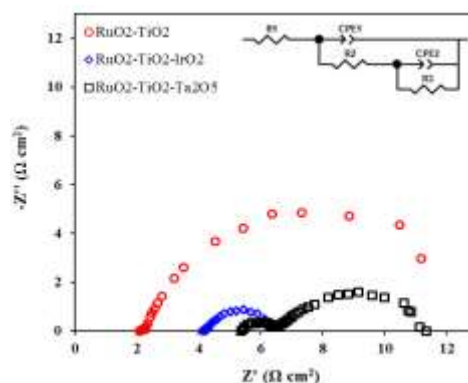


Figure 8. Nyquist diagrams of the coatings prepared with sol gel procedure and annealing at 450°C achieved at -0.85 V vs. SCE in a 1 mol L⁻¹ NaOH solution.

It lies in the range between 0 and 1 and how much it tends to 1 then the electrochemical behavior of electrode approaches the ideal capacitor properties.

$$T = C_{dl}^n (R_s^{-1} + R_{ct}^{-1})^{1-n}$$

(5) The fitting results are reported in table 1.

According to the results, the resistance of coating in the case of the coating containing IrO₂ is 0.12 Ω cm² and slightly is lower than RuO₂-TiO₂. It is because of replacement of 20 mol. % of low conductive material, TiO₂, with more conductive IrO₂.

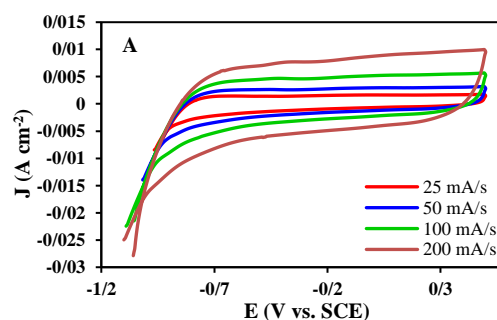
Table 1. EIS data fitting results for A) RuO₂-TiO₂ (20-80), B) RuO₂-TiO₂-IrO₂ (20-60-20), C) RuO₂-TiO₂-Ta₂O₅ (20-60-20) mol. % coatings.

Electrode	A	B	C
R _s (Ω cm ²)	2.08	4.13	5.32
R _f (Ω cm ²)	0.13	0.12	1.24
T (Ω ⁻¹ cm ⁻² s ^r)	0.1259	0.2012	0.1375

n_2	0.89	0.79	0.72
R_{ct} ($\Omega \text{ cm}^2$)	11.66	2.27	4.88

Contrariwise $\text{RuO}_2\text{-TiO}_2\text{-Ta}_2\text{O}_5$ coating has much higher film resistance in comparison with the two others. It arises from the replacement of 20 mol. % of RuO_2 with Ta_2O_5 which has poor crystallinity furthermore it is intrinsically poor conductive in comparison with IrO_2 and RuO_2 [37]. The n values also obtained by EIS measurements implicates on more porosity at the surface of $\text{RuO}_2\text{-TiO}_2\text{-Ta}_2\text{O}_5$ electrode. As said previously n lies in the range of 0 and 1 and how much its value be inclined to 1 the electrode has more uniform and smooth surface and its behavior is similar to ideal capacitor [38]. The value of n for the coating containing Ta_2O_5 is 0.72 which is a little lower than that of $\text{RuO}_2\text{-TiO}_2\text{-IrO}_2$. The results are in agreement with SEM micrographs. Charge transfer resistance value is the key kinetic parameter of such systems. R_{ct} has the lowest value at $\text{RuO}_2\text{-TiO}_2\text{-IrO}_2$ coating. The value of R_{ct} corresponding to $\text{RuO}_2\text{-TiO}_2$ is $11.66 \Omega \text{ cm}^2$. The obtained R_{ct} for $\text{RuO}_2\text{-TiO}_2\text{-Ta}_2\text{O}_5$ is $4.88 \Omega \text{ cm}^2$. The observed decreasing in R_{ct} can be related to the effect of roughness. Although $\text{RuO}_2\text{-TiO}_2$ coating has 20 mol. % more RuO_2 as electrocatalyst material but the surface roughness of $\text{RuO}_2\text{-TiO}_2\text{-Ta}_2\text{O}_5$ is more than $\text{RuO}_2\text{-TiO}_2$ coating. However in a given electrochemical reaction; intrinsic activity and surface roughness control the kinetics of reaction together. So the rougher electrode must have better kinetics. IrO_2 also is included in good catalyst materials for HER. Its catalytic activity toward HER is comparable to RuO_2 . Nevertheless the coating $\text{RuO}_2\text{-TiO}_2\text{-IrO}_2$ should be the best catalyst for HER in the present study because when it compares to $\text{RuO}_2\text{-TiO}_2$ coating it has more surface roughness considering n values and when compares to $\text{RuO}_2\text{-TiO}_2\text{-Ta}_2\text{O}_5$ coating it has 20 mol.% more electrocatalytic material. Cyclic voltammetry studies

for three different kinds of mixed metal oxide coatings were conducted at different scan rates of potential in 1mol.L^{-1} NaOH at 25°C . The results are presented in figure 9. All of the curves have characteristic shape of catalytic materials including RuO_2 which has been described at literature [23, 39]. Figure 9A and 9C are related to $\text{RuO}_2\text{-TiO}_2$ and $\text{RuO}_2\text{-TiO}_2\text{-Ta}_2\text{O}_5$ coatings respectively. As can be seen in these figures only two distinguishable peaks exist at forward and backward scan. The peak near to -0.1V is related to $\text{Ru (III) / Ru (IV)}$ and the other at zero is related to Ru (IV) / Ru (VI) redox couple. In figure 9B the other peak reveals at near to 0.3V which can be associated to IrO_2 . However the considered peaks disappear at higher scan rates and turn into one abroad peak. The voltammetric charge nominated as q^* is one beneficial parameters in voltammetry studies of electrocatalysts. It can be obtained by integration of voltammogram at a given potential range that could be considered as whole redox transition potential range [39, 40]. The value of q^* is proportional to the number of active sites. In the present work the anodic part of q^* was obtained in potential range of -0.5 to 0.1V vs. SCE at scan rate of 25mV s^{-1} . When the scan rate increases the number of surface sites contributed in the reaction decrease Because of fast scrolling of potential from HER limited area.



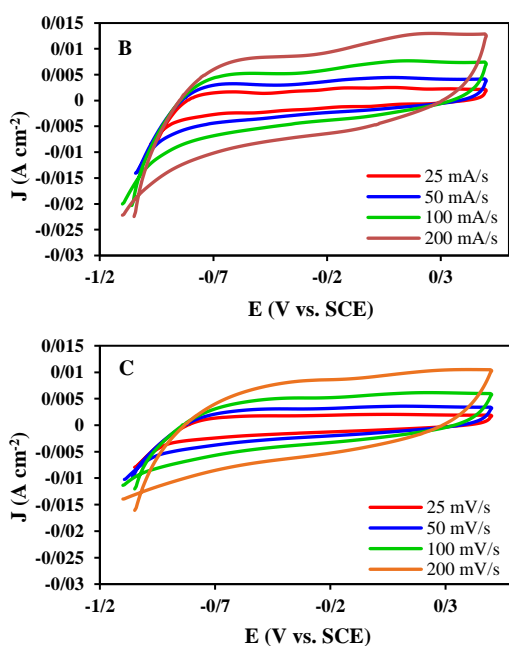


Figure 9. Cyclic voltammetry curves of A) RuO₂-TiO₂ (20-80), B) RuO₂-TiO₂-IrO₂ (20-80-20), C) RuO₂-TiO₂-Ta₂O₅ (20-80-20) mol. % coatings achieved at different scan rates of 25, 50, 100 and 200 mA s⁻¹ in a 1 mol L⁻¹ NaOH solution.

The longer period of time that potential rests at HER exclusive potentials (low scan rates) leads to more contribution of surface sites at the reaction but whatever it become shorter (high scan rates) only the sites are participated which are adjacent to the electrolyte. Nevertheless 25 mA cm⁻¹ is a good choice for determination of q*. The results of q* are provided at table 2. The coating containing IrO₂ has the highest amount of voltammetric charge which is 1.2 times bigger than that of RuO₂-TiO₂-Ta₂O₅ and 2.06 times than RuO₂-TiO₂. The obtained results of q* can be justified through the electrocatalytic material amount and roughness of surface. In the case of RuO₂-TiO₂-IrO₂ coating according to the SEM micrographs surface roughness has an important effect. On the other hand it has 20 mol. % more catalytic material than the two other coatings. Then, it also has the highest voltammetric charge. RuO₂-TiO₂-Ta₂O₅ is in the second place.

Table 2. Voltammetric charge values for A) RuO₂-TiO₂ (20-80), B) RuO₂-TiO₂-IrO₂ (20-60-20), C) RuO₂-TiO₂-Ta₂O₅ (20-60-20) mol. % coatings in potential range of -0.6 V to 0.5 V vs. SCE at the scan rate of 25 mV s⁻¹.

Electrode	A	B	C
q* (mC cm ⁻²)	30.59	62.99	51.97

The amount of catalytic material means RuO₂ in RuO₂-TiO₂-Ta₂O₅ coating is equal with RuO₂-TiO₂ coating. But the roughness of surface at former case is more than later. Nevertheless the binary coating of RuO₂-TiO₂ with the lowest roughness and low catalytic material has the lowest q*. Another parameter which is extracted from cyclic voltammograms is C_{dl}. It is well known as the capacitance of double layer or the charge accumulated at the electrical double layer without any contribution of faradaic reactions. Electrical double layer capacitance as voltammetric charge is in direct proportion with active surface area according to equation (6).

$$C = \epsilon \frac{A}{D} \tag{6}$$

Where ϵ is dielectric constant in F m⁻¹, A is the capacitor plates surface area in m², D is the separation between the plates in m and C is the capacitance in F [41]. The capacitance measurement was conducted through the capacitive current density vs. scan rate curves. The current densities at these curves were achieved from the regions of voltammograms which have no faradaic peaks as much as possible [42]. The obtained points were fitted to suitable lines that are presented in figure 10. As can be seen in this figure the slope of line is highest for RuO₂-TiO₂-IrO₂ coating which represents the most double layer capacitance in it. Both of RuO₂ and IrO₂ are favorable materials in supercapacitor technology. They have not only promising pseudocapacitance due to the high strength in water adsorption (eq. 1) but also suitable electronic structure for double layer capacitors [28,29,42]. Although the amount of catalytic material in both RuO₂-TiO₂ and RuO₂-TiO₂-Ta₂O₅ coatings

are similar, the higher roughness at later case has led to more double layer capacitance in it.

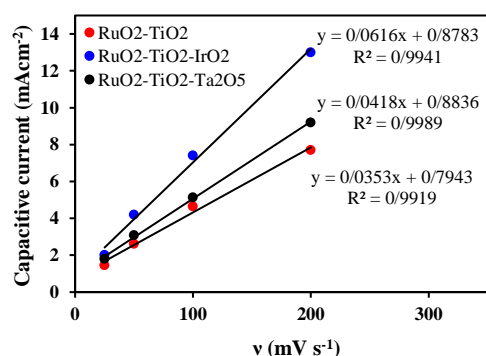


Figure 10. Capacitive current density vs. scan rate for the coatings prepared with sol gel procedure and annealing at 450°C.

For a more exact investigation of surface roughness, it is calculated via obtained values of C_{dl} for coatings and a reference value (eq. 7). Since the electrochemically deposited RuO₂ film takes place as a mediator thin film for improving the catalytic performance of all three electrodes then the primary roughness of electrodes depend on the surface of Ni substrate. So the double layer capacitance value of metallic Ni (20 μ F. cm⁻²) was considered as reference value. Similar method has been utilized to calculation of surface roughness factor by many authors [20, 38]. The roughness factor (R_f) is a unit less parameter that can be achieved by dividing the double layer capacitance values of coatings to that of Ni substrate. The results are exhibited at table 3.

$$R_f = \frac{C_{dl}}{20\mu F \text{ cm}^{-2}}$$

(7) The numerator part of eq. 7 is the double layer capacitance value which was extracted from capacitive current density vs. scan rate curves (figure 10) and 20 μ F cm⁻² is the double layer capacitance of smooth metallic Ni substrate. The ratio of obtained R_f values are similar to the ratio between q^* results. The higher R_f that is observed for RuO₂-TiO₂-IrO₂ coating implies the more accessible surface sites at same coating participated at HER.

Table 3. Roughness factor values for A) RuO₂-TiO₂ (20-80), B) RuO₂-TiO₂-IrO₂ (20-60-20), C) RuO₂-TiO₂-Ta₂O₅ (20-60-20) mol. % coatings.

Electrode	A	B	C
R_f	1765	3080	2090

Complementary evaluation of the activity of sol-gel derived and thermally decomposed at 450°C coatings were done through polarization studies in a 1mol L⁻¹ NaOH solution at the scan rate of 1mV s⁻¹. Tafel polarization curves are shown at figure 11. The slope of curves at the range of current density equal to (0.001-0.01) A cm⁻² considered as the low current densities tafel slope that are illustrated at table 4.

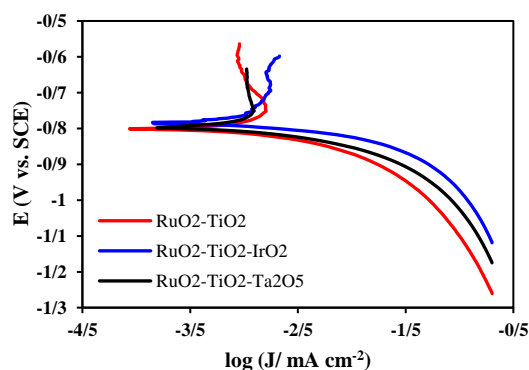


Figure 11. Tafel polarization curves of the coatings prepared with sol gel procedure and annealing at 450°C obtained in 1 mol L⁻¹ NaOH at the scan rate of 1 mV s⁻¹.

Considering the values of table 4, the coating containing 20 mol. % IrO₂ has the lowest tafel slope equal to 31mV dec⁻¹. The coating which contains 20 mol. % Ta₂O₅ has the slope of 47 mV dec⁻¹ and binary coating of RuO₂-TiO₂ (20-80) mol. % has the highest tafel slope equal to 60 mV dec⁻¹.

Table 4. Electrochemical activity parameters including $E_{100mA \text{ cm}^{-2}}$ and J_{100mV} for A) RuO₂-TiO₂ (20-80), B) RuO₂-TiO₂-IrO₂ (20-60-20), C) RuO₂-TiO₂-Ta₂O₅ (20-60-20) mol. % coatings extracted from linear sweep voltammetry curves.

Electrode	A	B	C
Tafel slope (mV dec ⁻¹)	31	47	60
$E_{100mA \text{ cm}^{-2}}$ (V)	-1.1	-0.973	-1.028
J_{100mV} (mA cm ⁻²)	-52.29	-118.6	-82.76

The results are in agreement with the literature in which the observed tafel slope for pure RuO₂ is 40-50 mV dec⁻¹ for low current densities and 230-240 mV dec⁻¹ at high current densities. is 240 mV dec⁻¹ and for pure IrO₂ is 120 mV dec⁻¹ [36]. Also for pure IrO₂ the slopes of 40 mV dec⁻¹ at low and 120 mV dec⁻¹ at high current densities have been reported [43]. The activity of pure IrO₂ is a little better than pure RuO₂ in alkaline solutions. Tafel polarization curves of noble metal oxide coatings of RuO₂ and IrO₂ either in pure or mixed together or other metal oxides like Ta₂O₅ and TiO₂ display two step at their cathodic sweep. Based on proposition of chen et al. volmer-heyrovsky mechanism governs at the process with these values of tafel slopes. The small tafel slope of RuO₂-TiO₂-IrO₂ (20-60-20) mol. % coating at lower current densities ($\eta=50$ mV) confirm the influence of addition of 20 mol. % IrO₂. It seems addition of IrO₂ leads to formation of solid solution between RuO₂ and IrO₂ which both have similar crystallographic structure and through this effect it influences on the strength of the bond among the adsorbing H and the surface active sites. Finally the change in strength of adsorption bond of M-H affects the mechanism of HER. In the field of hydrogen evolution reaction, the activity assessment curves known as volcano depicts relationship between observed current density (representative of the kinetic activity) against M-H adsorption bond strength [44]. According to these curves whatever the strength of M-H bond falls in the range of low values there is poor kinetics because of the low adsorption. On the other hand whatever the bond is strength then its breaking at the next stage (desorption stage) will be needed to more activation energy [11]. Nevertheless the bonds with mediocre strength should have fast kinetics as can be concluded from volcano curves at the literature. Figure 12 presents linear sweep voltammetry curves of the coatings obtained in a 1 mol L⁻¹ NaOH solution at the scan rate of 1 mV s⁻¹ and room temperature. The horizontal part of the curves at the potentials more

positive than -0.8V are relevant to the capacitive current. Afterward the faradaic current reveals and current density commence to increase. As can be seen in figure 12 the onset potentials (the potential of commence of faradaic reaction) are almost similar at all the coatings. The main difference among the curves lies in the slope of them at their faradaic region. Linear sweep voltammetry more accurately disclose the slope of increasing of current density by increasing in the applied potential. Anyway at equal overpotentials the more current density means the better kinetics. As a supplementary assessment the observed current density at -1V vs. SCE as well as the needed overpotential at the current density of 100 mA cm⁻² was extracted from linear sweep voltammetry curves (figure 12) that are presented at table 4.

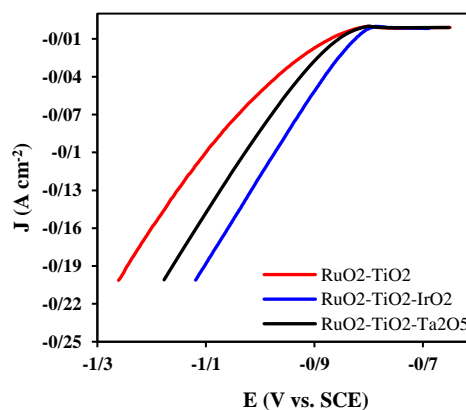


Figure 12. Linear sweep voltammetry curves for the coatings prepared with sol gel procedure and annealing at 450°C obtained in 1 mol L⁻¹ NaOH at the scan rate of 1 mV s⁻¹.

According to results of table 4 the potential needed to observing of 100 mA cm⁻² current density is the minimum value for RuO₂-TiO₂-IrO₂ coating. Also the highest current density equal to 118.6 mA cm⁻² at the applied potential of -1V vs. SCE is observed for same coating. As said previously the more activity at the case of RuO₂-TiO₂-IrO₂ originates not only from the more surface roughness but also direct contribution of IrO₂ at HER. In the case of RuO₂-TiO₂-Ta₂O₅ the relatively better kinetics in comparison with RuO₂-TiO₂ comes from just the more surface roughness of it.

3.2.3 Accelerated Service life test of Ni/RuO₂/RuO₂-TiO₂, Ni/RuO₂/RuO₂-TiO₂-IrO₂, Ni/RuO₂/RuO₂-TiO₂-Ta₂O₅ electrodes

Stability of sol gel derived and thermally decomposed at 450°C coatings of RuO₂-TiO₂ (20-80), RuO₂-TiO₂-IrO₂ (20-60-20) and RuO₂-TiO₂-Ta₂O₅ (20-60-20) mol. % were evaluated in a motionless 2mol L⁻¹ NaOH solution under constant current density of 400mA cm⁻². With respect to the results of the test which are presented at the form of E_w-Time curve in figure 13 the potential of electrodes at the beginning time of test are different. That difference arises from the difference in abundance of the accessible surface sites (roughness factor) because in the beginning time at which there is no penetration of electrolyte through the coatings into their inner layers yet, surface accessible sites are responsible to HER. After near 8 hours the potential of working electrode (the electrode which contains coating) drops to 1.4V vs. SCE. This potential drop originates from penetration of electrolyte to the inner layers of coating that exposes inner sites to HER [22].

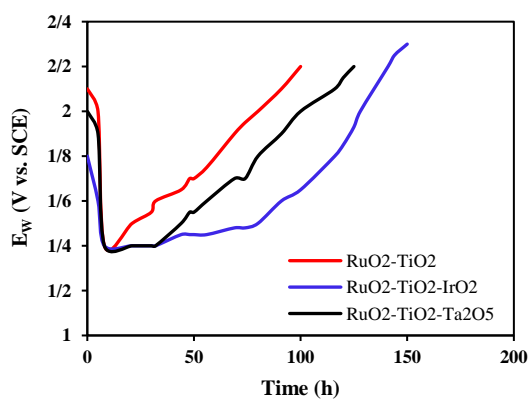


Figure 13. E_w-Time curves for the coatings prepared with sol gel procedure and annealing at 450°C obtained via electrolysis under constant current density of 400 mA cm⁻² in 2 mol L⁻¹ NaOH at room temperature.

Interestingly at the end of 8hours the potential of all three electrodes are equal to 1.4V. It indicates that the number of inner sites is very much more than surface sites so that the difference in surface sites becomes negligible. At the following hours the potential

immediately increases for RuO₂-TiO₂ coating by a relatively constant slope. But this increasing postpones near 24 hours for RuO₂-TiO₂-Ta₂O₅ and 72 hours for RuO₂-TiO₂-IrO₂ coating. However there is a slight enhancement at the potential at these two intervals. This observation can be explained by the stabilizing effect of IrO₂ and Ta₂O₅ on RuO₂ through the formation of solid solution structures. After 24 and 72 hours of operating time respectively for RuO₂-TiO₂-Ta₂O₅ and RuO₂-TiO₂-IrO₂ coatings the potential commences to increasing at both of them and reaches to 2.2V vs. SCE after 93 hours for RuO₂-TiO₂-Ta₂O₅ and 67 hours for RuO₂-TiO₂-IrO₂ coating. At the potential enhancement region of curves through the reduction of active materials including RuO₂ and IrO₂ as soluble species of Ru³⁺ and Ir³⁺ and releasing to the electrolyte the active sites demolishes [45]. Another critical reason of destruction of such electrodes in alkaline mediums is the chemisorption of H inside the coating that leads to formation of hydrogen in inner layers and finally swelling and detachment of coating. Totally it can be concluded that since the RuO₂-TiO₂-IrO₂ (20-60-20) coating has more active sites then it takes more time to be deactivated. In the RuO₂-TiO₂-Ta₂O₅ as XRD pattern shows some of Ta₂O₅ is involved in solid solution structure with RuO₂. The residual part stays in amorphous form of Ta₂O₅ and provides more stability to its own coating in comparison with RuO₂-TiO₂. Finally the RuO₂-TiO₂ coating with lower active sites has the lowest stability in accelerated stability test.

4. Conclusion

In the present work Ni/RuO₂ electrode were synthesized with electrochemical deposition of hydroxide and peroxide of ruthenium from RuCl₃ bath and then thermal treatment at 120°C for 15min. SEM micrographs revealed a relatively mud-cracked structure. Based on cyclic and linear sweep voltammetry investigations conducted on Ni bare and

Ni/RuO₂ prepared with electrochemical deposition-heat treatment at 120°C, Ni/RuO₂ has much more activity toward HER according to observed compressed water oxidation/reduction potential window with high current density at all applied potentials as well as the large slope of current density-potential at linear sweep voltammogram. Electrochemically prepared Ni/RuO₂ electrode was used as new substrate and three different kinds of mixed metal oxide coatings fabricated by a combinational method encompasses sol gel and thermal decomposition at 450°C. SEM micrographs indicated more roughness for the coatings containing (20 mol. %) of IrO₂ and Ta₂O₅. Double layer capacitance values which were obtained by cyclic voltammetry studies were used to measurement of roughness factor. The more surface roughness was achieved for the coating containing 20 mol. % IrO₂. Due to the high roughness the adsorption of water and consequently electrocatalytic activity increases. Polarization studies also revealed the best kinetic parameters for the coating containing IrO₂ by the lowest tafel slope of 31mV dec⁻¹. As a result of superior stabilizing influence of IrO₂ and RuO₂ to each other beside the more surface active sites the best stability time was observed for RuO₂-TiO₂-IrO₂ coating. However based on literature Ta₂O₅ has also stabilizing effect at the mixed metal oxide structures.

Acknowledgments

The authors would like to appreciate the Research Vice-Chancellor Office of Tabriz University for their supports.

References

- [1] P. Hoffmann, Tomorrow's energy: hydrogen, fuel cells, and the prospects for a cleaner planet: MIT press, 2012.
- [2] J. Romm, The car and fuel of the future, *Energy Policy*, 34 (2006) 2609-2614.
- [3] M. Balat, Potential importance of hydrogen as a future solution to environmental and transportation problems, *Int. J. Hydrogen Energy*, 33 (2008) 4013-4029.
- [4] J.D. Holladay, J. Hu, D.L. King, Y. Wang, An overview of hydrogen production technologies, *Catal. Today*, 139 (2009) 244-260.
- [5] T. Rostrup-Nielsen, Manufacture of hydrogen, *Cataly. Today*, 106 (2005) 293-296.
- [6] J. Turner, G. Sverdrup, M.K. Mann, P.C. Maness, B. Kroposki, M. Ghirardi, et al., Renewable hydrogen production, *Int. J. Energy Res.*, 32 (2008) 379-407.
- [7] K. Zeng, D. Zhang, Recent progress in alkaline water electrolysis for hydrogen production and applications, *Prog. Energy Combust. Sci.*, 36 (2010) 307-326.
- [8] S. Marini, P. Salvi, P. Nelli, R. Pesenti, M. Villa, M. Berrettoni, et al., Advanced alkaline water electrolysis, *Electrochim. Acta*, 82 (2012) 384-391.
- [9] M. Carmo, D.L. Fritz, J. Mergel, D. Stolten, A comprehensive review on PEM water electrolysis, *Int. J. Hydrogen Energy*, 38 (2013) 4901-4934.
- [10] J. Barber, S. Morin, B. Conway, Specificity of the kinetics of H₂ evolution to the structure of single-crystal Pt surfaces, and the relation

- between opd and upd H, J. Electroanal. Chem, 446(1998) 125-138.
- [11] N. Danilovic, R. Subbaraman, D. Strmcnik, V.R. Stamenkovic, N.M. Markovic, Electrocatalysis of the HER in acid and alkaline media, J. Serb. Chem. Soc., 78 (2013) 2007-2015.
- [12] A. Matsuda, R. Notoya, Hydrogen overvoltage on platinum in aqueous sodium hydroxide: part 1. Rate of the Discharge Step, J. Res. Inst. Catal., Hokkaido Univ., 14 (1966) 165-191.
- [13] N. Krstajić, V. Jović, L. Gajić-Krstajić, B. Jović, A. Antozzi, G. Martelli, Electrodeposition of Ni–Mo alloy coatings and their characterization as cathodes for hydrogen evolution in sodium hydroxide solution, Int. J. Hydrogen Energy, 33 (2008) 3676-3687.
- [14] R.K. Shervedani, A.R. Madram, Kinetics of hydrogen evolution reaction on nanocrystalline electrodeposited Ni₆₂Fe₃₅C₃ cathode in alkaline solution by electrochemical impedance spectroscopy, Electrochim. Acta, 53 (2007) 426-433.
- [15] L. Birry, A. Lasia, Studies of the hydrogen evolution reaction on Raney nickel-molybdenum electrodes, J. Appl. Electrochem., 34 (2004) 735-749.
- [16] D. Miousse, A. Lasia, V. Borck, Hydrogen evolution reaction on Ni-Al-Mo and Ni-Al electrodes prepared by low pressure plasma spraying, J. Appl. Electrochem., 25 (1995) 592-602.
- [17] P. Los, A. Lasia, Electrocatalytic properties of amorphous nickel boride electrodes for hydrogen evolution reaction in alkaline solution, J. Electroanal. Chem., 333 (1992) 115-125.
- [18] A. Vijh, G. Bélanger, R. Jacques, Electrolysis of water on silicides of some transition metals in alkaline solutions, Int. J. Hydrogen Energy, 17 (1992) 479-483.
- [19] Y. Li, H. Wang, L. Xie, Y. Liang, G. Hong, H. Dai, MoS₂ nanoparticles grown on graphene: an advanced catalyst for the hydrogen evolution reaction, J. Am. Chem. Soc., 133 (2011) 7296-7299.
- [20] S. Shibli, V. Dilimon, Development of TiO₂-supported nano-RuO₂-incorporated catalytic nickel coating for hydrogen evolution reaction, Int. J. Hydrogen Energy, 33 (2008) 1104-1111.
- [21] J. Cheng, H. Zhang, H. Ma, H. Zhong, Y. Zou, Study of carbon-supported IrO₂ and RuO₂ for use in the hydrogen evolution reaction in a solid polymer electrolyte electrolyzer, Electrochim. Acta, 55 (2010) 1855-1861.
- [22] I. Kodintsev, S. Trasatti, Electrocatalysis of H₂ evolution on RuO₂+IrO₂ mixed oxide electrodes,

- Electrochim. Acta, 39 (1994) 1803-1808.
- [23] D. Miousse, A. Lasia, Hydrogen evolution reaction on RuO₂ electrodes in alkaline solutions, *J. New Mater. Electrochem. Syst.*, 2 (1999) 71-78.
- [24] C. Angelinetta, S. Trasatti, L.D. Atanososka, R. Atanososki, Surface properties of RuO₂+ IrO₂ mixed oxide electrodes, *J. Electroanal. Chem. Interfacial electrochem.*, 214 (1986) 535-546.
- [25] L. Chen, D. Guay, A. Lasia, Kinetics of the Hydrogen Evolution Reaction on RuO₂ and IrO₂ Oxide Electrodes in H₂SO₄ Solution: An AC Impedance Study, *J. Electrochem. Soc.*, 143 (1996) 3576-3584.
- [26] E. Kötzt, S. Stucki, Ruthenium dioxide as a hydrogen-evolving cathode, *J. Appl. Electrochem.*, 17 (1987) 1190-1197.
- [27] J. Boodts, S. Trasatti, Hydrogen evolution on iridium oxide cathodes, *J. Appl. Electrochem.*, 19 (1989) 255-262.
- [28] N. Spataru, J.G. Le Helloco, R. Durand, A study of RuO₂ as an electrocatalyst for hydrogen evolution in alkaline solution, *J. Appl. Electrochem.*, 26 (1996) 397-402.
- [29] C.C. Hu, M.J. Liu, K.H. Chang, Anodic deposition of hydrous ruthenium oxide for supercapacitors, *J. Power Sources*, 163 (2007) 1126-1131.
- [30] N. Yoshida, Y. Yamada, S.I. Nishimura, Y. Oba, M. Ohnuma, A. Yamada, Unveiling the Origin of Unusual Pseudocapacitance of RuO₂.nH₂O from Its Hierarchical Nanostructure by Small-Angle X-ray Scattering, *J. Phys. Chem. C*, 117 (2013) 12003-12009.
- [31] I. Kodintsev, S. Trasatti, M. Rubel, A. Wieckowski, N. Kaufher, X-ray photoelectron spectroscopy and electrochemical surface characterization of iridium (IV) oxide+ruthenium (IV) oxide electrodes, *Langmuir*, 8 (1992) 283-290.
- [32] Z. Yi, C. Kangning, W. Wei, J. Wang, S. Lee, Effect of IrO₂ loading on RuO₂-IrO₂-TiO₂ anodes: a study of microstructure and working life for the chlorine evolution reaction, *Ceram. Int.*, 33 (2007) 1087-1091.
- [33] V. Natarajan, S. Basu, Performance and degradation studies of RuO₂-Ta₂O₅ anode electrocatalyst for high temperature PBI based proton exchange membrane water electrolyser, *Int. J. Hydrogen Energy*, 40 (2015) 16702-16713.
- [34] G. Vercesi, J.Y. Salamin, and C. Comninellis, Morphological and microstructural the Ti/IrO₂-Ta₂O₅ electrode: effect of the preparation temperature, *Electrochim. Acta*, 36 (1991) 991-998.
- [35] H. Over, Surface chemistry of ruthenium dioxide in heterogeneous

- catalysis and electrocatalysis: from fundamental to applied research, *Chem. Rev.*, 112 (2012) 3356-3426.
- [36] A. Cornell, D. Simonsson, Ruthenium dioxide as cathode material for hydrogen evolution in hydroxide and chlorate solutions, *J. Electrochem. Soc.*, 140 (1993) 3123-3129.
- [37] A.T. Marshall, S. Sunde, M. Tsyppkin, R. Tunold, Performance of a PEM water electrolysis cell using $\text{Ir}_x\text{Ru}_y\text{Ta}_z\text{O}_2$ electrocatalysts for the oxygen evolution electrode, *Int. J. Hydrogen Energy*, 32 (2007) 2320-2324.
- [38] U. Lačnjevac, B. Jović, V. Jović, V. Radmilović, N. Krstajić, Kinetics of the hydrogen evolution reaction on Ni-(Ebonex-supported Ru) composite coatings in alkaline solution, *Int. J. Hydrogen Energy*, 38 (2013) 10178-10190.
- [39] T.C. Wen, C.C. Hu, Hydrogen and Oxygen Evolutions on Ru-Ir Binary Oxides, *J. Electrochem. Soc.*, 139 (1992) 2158-2163.
- [40] R. Savinell, R. Zeller, J. Adams, Electrochemically active surface area voltammetric charge correlations for ruthenium and iridium dioxide electrodes, *J. Electrochem. Soc.*, 137 (1990) 489-494.
- [41] E. Frackowiak, F. Beguin, Carbon materials for the electrochemical storage of energy in capacitors, *Carbon*, 39 (2001) 937-950.
- [42] B.O. Park, C. Lokhande, H.S. Park, K.D. Jung, O.S. Joo, Electrodeposited ruthenium oxide (RuO_2) films for electrochemical supercapacitors, *J. Mater. Sci.*, 39 (2004) 4313-4317.
- [43] H. Chen, S. Trasatti, Cathodic behaviour of IrO_2 electrodes in alkaline solution: Part 2. Kinetics and electrocatalysis of H_2 evolution, *J. Electroanal. Chem.*, 357 (1993) 91-103.
- [44] J.K. Nørskov, T. Bligaard, A. Logadottir, J. Kitchin, J. Chen, S. Pandalov, et al., Trends in the exchange current for hydrogen evolution, *J. Electrochem. Soc.*, 152 (2005) J23-J26.
- [45] Y. Mo, W.B. Cai, J. Dong, P.R. Carey, D.A. Scherson, In situ surface enhanced Raman scattering of ruthenium dioxide films in acid electrolytes, *Electrochem. Solid-State Lett.*, 4 (2001) E37-E38.

